Bridging the Gap Between TLM and FDTD

Channabasappa Eswarappa, *Member, IEEE,* and Wolfgang J. R. Hoefer, *Fellow, IEEE*

***Abstract*—A real-time interface between transmission line modeling (TLM) and finite difference time domain (FDTD) algorithms has been developed and validated. A structure can be subdivided in an arbitrary manner into connected TLM and FDTD subdomains that are updated simultaneously. In this way the specific advantages of both methods can be exploited when solving a given problem. The interface procedure has been validated by solving identical structures, first with TLM, then FDTD, and finally with a combination of both. All three methods yield identical numerical results for equal excitation, space, and time resolution.**

I. Introduction

SEVERAL papers have been published on the common features as well as on the differences of TLM and FDTD algorithms [1]–[5]. Both techniques are extensively used to analyze electromagnetic structures of arbitrary geometry. FDTD is heavily favored by the radiation and scattering community, while TLM is used mostly by researchers interested in guided propagation problems. However, the actual combination of these techniques in a real-time analysis procedure has not yet been described. In this letter, the technique for combining TLM and FDTD will be reported and validated for the two-dimensional case, assuming the properties of free space.

II. Theory

TLM and FDTD algorithms have been extensively published in the literature. However, since their interfacing requires a certain consistency in their formulation, both will be repeated here for convenience.

Maxwell's equations for $\frac{\partial}{\partial z} = 0, E_x = E_y = H_z = 0$ discretized with central finite differences are, according to Yee [6]

$$H_x^{n+\frac{1}{2}}\left(i,j+\frac{1}{2}\right) = H_x^{n-\frac{1}{2}}\left(i,j+\frac{1}{2}\right) - B\big(E_z^n(i,j+1) - E_z^n(i,j)\big) \quad (1a)$$

$$H_y^{n+\frac{1}{2}}\left(i+\frac{1}{2},j\right) = H_y^{n-\frac{1}{2}}\left(i+\frac{1}{2},j\right) + B\big(E_z^n(i+1,j) - E_z^n(i,j)\big) \quad (1b)$$

$$E_z^{n+1}(i,j) = E_z^n(i,j) + A\left(H_y^{n+\frac{1}{2}}\left(i+\frac{1}{2},j\right) - H_y^{n+\frac{1}{2}}\left(i-\frac{1}{2},j\right)\right) - A\left(H_x^{n+\frac{1}{2}}\left(i,j+\frac{1}{2}\right) - H_x^{n+\frac{1}{2}}\left(i,j-\frac{1}{2}\right)\right) \quad (1c)$$

where $A = \frac{\Delta t}{\varepsilon_0 \Delta l}$, $B = \frac{\Delta t}{\mu_0 \Delta l}$. i, j, and n are normalized space and time coordinates.

E and H fields are separated in space by $\Delta l/2$ [see Fig. 1(a)] and are evaluated at alternate half-time steps. On the other hand, a 2-D shunt TLM algorithm [a unit cell is shown in Fig. 1(b)] consists of the following scattering and transfer events relating the reflected to the incident voltage impulses:

$$_r[V]^{n+\frac{1}{2}} = [S]\,_i[V]^{n-\frac{1}{2}}; \quad _i[V]^{n+\frac{1}{2}} = [C]\,_r[V]^{n+\frac{1}{2}} \quad (2)$$

where $[S]$ is the scattering matrix and $[C]$ is the connection matrix. The equivalences between the field components in FDTD and the TLM voltage impulses are

$$E_z^n(i,j) \equiv V_z^n(i,j) = \frac{1}{2}\,_{\text{inc}}[V_1(i,j) + V_2(i,j) + V_3(i,j) + V_4(i,j)]^{n-\frac{1}{2}} \quad (3a)$$

$$H_x^{n+\frac{1}{2}}\left(i,j+\frac{1}{2}\right) \equiv I_y^{n+\frac{1}{2}}\left(i,j+\frac{1}{2}\right) = \frac{1}{Z_l}\,_{\text{ref}}[V_3(i,j) - V_1(i,j+1)]^{n+\frac{1}{2}} \quad (3b)$$

$$H_y^{n+\frac{1}{2}}\left(i+\frac{1}{2},j\right) \equiv -I_x^{n+\frac{1}{2}}\left(i+\frac{1}{2},j\right) = \frac{1}{Z_l}\,_{\text{ref}}[V_2(i+1,j) - V_4(i,j)]^{n+\frac{1}{2}} \quad (3c)$$

where $Z_l = Z_0\sqrt{2}$ is the link line impedance. The subscripts 1–4 of the voltage impulses refer to the TLM branch numbers shown in Fig. 1(b). Note that in TLM, the magnetic field components are also available at the nodes at integer multiples of time steps, and the electric field can be sampled halfway between nodes at half time steps.

To make the TLM and FDTD algorithms compatible, the time step in FDTD must be chosen as

$$\Delta t = \Delta l/(\sqrt{2}c) \quad (4)$$

where c is the speed of light. When performing the two algorithms in parallel, scattering at the TLM nodes corresponds to the updating of the electric field in FDTD, and impulse

Manuscript received June 2, 1995. This work was supported by the Natural Sciences and Engineering Research Council of Canada, MPR Teltech Inc., the Science Council of British Columbia, and the University of Victoria.

The authors are with the Department of Electrical and Computer Engineering, University of Victoria, Victoria, B.C. V8W 3P6, Canada.

Publisher Item Identifier S 1051-8207(96)00456-4.

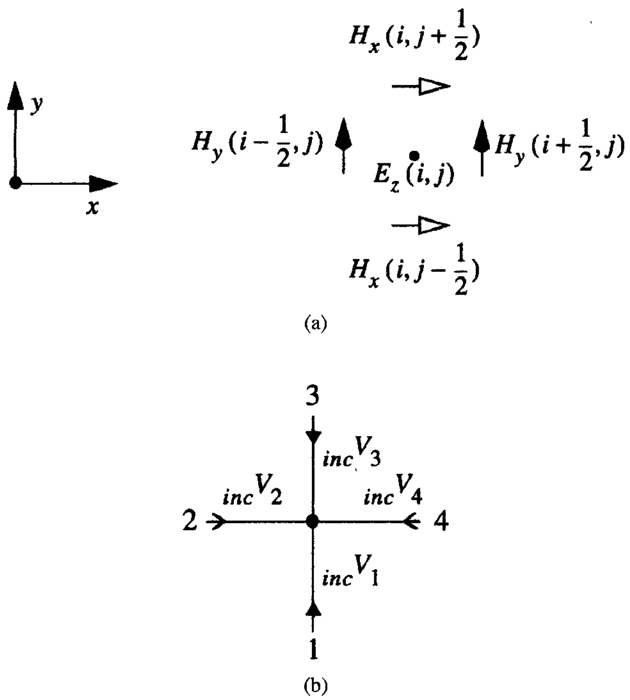

Fig. 1. (a) 2-D FDTD node. (b) 2-D shunt TLM node.

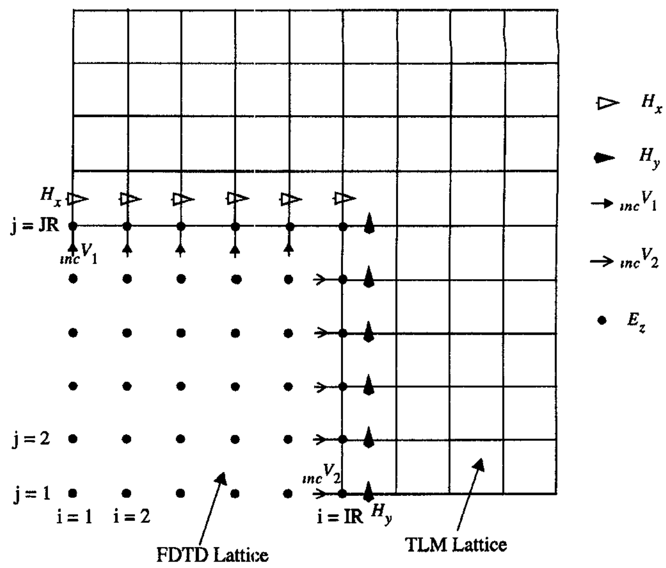

Fig. 2. Discretization of space with interconnected TLM and FDTD lattices. The two subdomains overlap by one cell width. The algorithms are coupled by equating two collocated field components in each common cell.

transfer between TLM cells corresponds to the updating of the magnetic field in FDTD.

In Fig. 2, a 2-D space is discretized partly with a FDTD mesh and partly with a shunt TLM mesh. The points shown in the FDTD lattice are the positions of the electric field samples E_z, while the lines shown in the TLM mesh represent the link transmission lines. The TLM shunt nodes are thus collocated with the E_z components in the FDTD scheme. Both subdomains overlap by one cell width Δl.

To implement scattering [see (2)] at the TLM nodes in the interface zone, we need to inject voltage impulses $_{\rm inc}V$ through their free branches from the FDTD subdomain. These impulses can be computed by forcing the node voltages to be equal to the E_z field values at these nodes obtained with the FDTD algorithm. For example, the impulses $_{\rm inc}V_1$ incident on the nodes at $j = JR$ can be obtained from (3a) by subtracting the other three voltage impulses from E_z at these points

$$\begin{aligned}{}_{\rm inc}V_1^{n-\frac{1}{2}}(i, JR) = 2E_z^n(i, JR) - {}_{\rm inc}[V_2(i, JR) \\ + V_3(i, JR) + V_4(i, JR)]^{n-\frac{1}{2}}. \quad (5)\end{aligned}$$

On the other hand, the execution of the FDTD algorithm in the interface region calls for the updating of the H_x values at $j = JR + 1/2$. These are obtained from the TLM voltages at the nodes in row $j = JR + 1$. Equation (1a) yields

$$\begin{aligned}&H_x^{n+\frac{1}{2}}\left(i, JR + \frac{1}{2}\right) \\ &= H_x^{n-\frac{1}{2}}\left(i, JR + \frac{1}{2}\right) \\ &\quad - B\left\{\frac{1}{2}\,{}_{\rm inc}[V_1(i, JR+1)\right. \\ &\quad + V_2(i, JR+1) + V_3(i, JR+1) \\ &\quad \left. + V_4(i, JR+1)]^{n-\frac{1}{2}} - E_z^n(i, JR)\right\} \quad (6)\end{aligned}$$

where $E_z(i, JR+1)$ has been set equal to the node voltage according to (3a).

Similarly, the incident voltage impulses $_{\rm inc}V_2$ on the branches 2 of the TLM interface nodes at $i = IR$ can be computed using the following equation:

$$\begin{aligned}{}_{\rm inc}V_2^{n-\frac{1}{2}}(IR, j) = 2E_z^n(IR, j) - {}_{\rm inc}[V_1(IR, j) \\ + V_3(IR, j) + V_4(IR, j)]^{n-\frac{1}{2}} \quad (7)\end{aligned}$$

and H_y in the interface region is updated as follows:

$$\begin{aligned}&H_y^{n+\frac{1}{2}}\left(IR + \frac{1}{2}, j\right) \\ &= H_y^{n-\frac{1}{2}}\left(IR + \frac{1}{2}, j\right) \\ &\quad + B\left\{\frac{1}{2}\,{}_{\rm inc}[V_1(IR+1, j) + V_2(IR+1, j)\right. \\ &\quad + V_3(IR+1, j) + V_4(IR+1, j)]^{n-\frac{1}{2}} \\ &\quad \left. - E_z^n(IR, j)\right\}. \quad (8)\end{aligned}$$

This completes the connection of the two algorithms.

III. Numerical Experiments and Results

In order to test the interface and the compatibility of the FDTD and TLM algorithms we have enclosed a 2-D computational space of 500×500 square cells with magnetic walls so that it could sustain fields at all frequencies, including dc. Three different methods were used to model this space:

Method A: Shunt-connected 2-D-TLM exclusively;
Method B: Yee's leapfrog 2-D-FDTD exclusively;

Method C: 2-D-TLM in one part, and 2-D-FDTD in the remaining part. Various ways of subdividing the space were tried, such as sandwiching a TLM subregion between two FDTD regions, surrounding a TLM island with a FDTD mesh, or simply dividing the space half into TLM and half into FDTD along one of the main axes.

The time response of all meshes to "impulsive excitations" at randomly selected input points was computed and compared. By "impulsive excitation" we mean the following:

In TLM, the node voltage at the source point is set equal to 1 V at $t = 0$. In FDTD, the electric field at the center of the source cell is set to 1 V/m at $t = 0$. The following observations were made in all numerical experiments without exception:

1) When the mixed mesh was excited in a TLM subregion, all three field components were identical in all cells (including the FDTD cells), and at all time steps, to those obtained in the exclusive TLM mesh with identical impulse excitation.
2) When the mixed mesh was excited in a FDTD subregion, all three field components were identical in all cells (including the TLM cells), and at all time steps, to those obtained in the exclusive FDTD mesh with identical impulse excitation.

These numerical experiments demonstrate that all field components travel seamlessly from one subdomain to the other in any direction, and that the numerical response of a composite mesh cannot be distinguished from that of an exclusive TLM or FDTD mesh, provided that the excitation is identical! In other words, if the excitation point is situated in a TLM region, the typical TLM response is imposed upon the connected FDTD mesh, and vice versa.

IV. Conclusion

An interface between 2-D shunt TLM and FDTD has been successfully developed and validated. Numerical solutions travel seamlessly between the two types of meshes, provided that identical space and time steps are used in both schemes. All electric field components at the cell centers and all magnetic field components tangential to the cell borders are identical in both schemes for identical excitation. The region containing the excitation point always imposes its own characteristic impulse response upon the other type of mesh connected to it.

The interfacing algorithm allows us to clearly confirm the common features and the differences between TLM and FDTD. Furthermore, it gives us the freedom of choosing the most appropriate discretization approach in different parts of the computational domain. For example, Berenger's FDTD perfectly matched layer (PML) absorbing boundary conditions [7] can easily be implemented in TLM through the interface, while Johns Matrix boundaries can be combined with a FDTD simulation. Future work will be directed toward hybrid FDTD-TLM modeling in three space dimensions.

References

[1] P. B. Johns, "On the relation between TLM and finite-difference methods for Maxwell's equations," *IEEE Trans. Microwave Theory Tech.*, vol. 35, no. 1, pp. 60–61, Jan. 1987.

[2] Z. Chen, M. M. Ney, and W. J. R. Hoefer, "A new finite-difference time-domain formulation and its equivalence with the TLM symmetrical condensed node," *IEEE Trans. Microwave Theory Tech.*, vol. 39, no. 12, pp. 2160–2169, Dec. 1991.

[3] M. Krumpholz and P. Russer, "A field theoretical derivation of TLM," *IEEE Trans. Microwave Theory Tech.*, vol. 39, no. 3, pp. 1660–1668, Sept. 1994.

[4] M. Celuch-Marcysiak and W. K. Gwarek, "A spurious TLM mode and its effect on the equivalence of the FDTD and TLM methods," in *URSI Radio Science Meet. Dig.*, Seattle, June 19–24, 1994, p. 98.

[5] H. Jin and R. Vahldieck, "Direct derivations of TLM symmetrical condensed node and hybrid symmetrical condensed node from Maxwell's equations using centered differencing and averaging," *IEEE Trans. Microwave Theory Tech.*, vol. 42, no. 12, pp. 2554–2561, Dec. 1994.

[6] K. S. Yee, "Numerical solution of initial boundary value problems involving Maxwell's equations," *IEEE Trans. Antennas Propagat.*, vol. 14, no. 3, pp. 302–307, May 1966.

[7] J.-P. Berenger, "A perfectly matched layer for the absorption of electromagnetic waves," *J. Computational Phys.*, vol. 114, pp. 185–200, 1994.